Investigation on the Growth of YVO_4 and Ce^{3+}-Doped YVO_4 Single Crystals

Shuai Wang[1,*], Yongfeng Ruan[2], Youfa Wang[2], Pengfei Wang[1]

[1]School of Science, Shandong Jiaotong University, Jinan 250357, China;

[2]School of Science, Tianjin University, Tianjin 300072, China.

*shuaiwangtju@163.com

Abstract

High-quality YVO_4 and Ce^{3+}-doped YVO_4 single crystals were grown by the Czochralski method. Based on the theoretical analysis, experimental equipment and experience, the optimal growth parameters have been obtained as follows: the axial gradient temperature is 7 K/mm, the growth rate is 1.5-2.0 mm/h, the crystal rotation speed is about 20-25 r/min, the final cooling rate is less than 15 K/h. The whole period of crystal growth is about 36 hours. The X-ray diffraction (XRD) patterns indicated that the obtained phase was YVO_4 without any parasitic phase.

Keywords

YVO_4; Czochralski; Temperature Gradient; Growth Rate; Cooling Rate; XRD.

1. Introduction

The compound of yttrium orthovanadate (YVO_4) doesn't chemically exist in nature. Goldschmidt and Haralden synthesized this compound firstly [1]. The pure YVO_4 and RE^{3+}-doped YVO_4 crystals have been heavily investigated and grown by the Czochralski (CZ), Bridgman-Stockbarger (B-Z), floating zone melting, flux, verneuil, etc. From 1960s, the size and quality of the crystal can not meet the need of application. For the mass-produced YVO_4 and RE^{3+}-doped YVO_4 crystals, the Czochralski method is proved to be most successful at present [2-4]. The Czochralski (Cz) pulling method has been well developed and widely applied to the field of crystal growth [5]. In this paper, the pure YVO_4 and Ce^{3+}-doped YVO_4 single crystals with different doping concentrations have been successfully grown by the Czochralski method in a medium frequency induction furnace. In order to obtain the high-quality single crystals, choosing the appropriate temperature gradient, growth rate and cooling rate plays a very important role in the crystal growth. On the basis of experiments and theoretical analyses, the optimal growth parameters were obtained. The X-ray diffraction patterns testified that all samples exhibited the pure tetragonal YVO_4 crystalline phase without any parasitic phases.

2. Experimental procedures

Fig. 1 shows the experimental equipment of crystal growth which is composed of vacuum device (a rotary and a diffusion pump) and growth chamber. The furnace designed for the crystal growth in the growth chamber is shown in Fig. 2. Pure YVO_4 and Ce^{3+}-doped YVO_4 crystals were grown by the Czochralski method in a medium frequency induction furnace. High-purity synthesized powders (>99.99%) of commercially available Y_2O_3, V_2O_5 and $Ce_2(CO_3)_3$ were applied to crystal growth. These raw materials were weighed and mixed in stoichiometric amounts. It is to be noticed that the Ce_2O_3 is unstable at room temperature. Generally, the CeO_2 is used as a raw material of Ce^{3+}-doped optical crystals in reducing atmosphere. Nevertheless, it can not rule out the possibility of some Ce^{4+} ions existing in crystals. In this work, the $Ce_2(CO_3)_3$ is used to grow the Ce^{3+}-doped YVO_4 crystals in nitrogen atmosphere, which is considered as the donor of Ce^{3+} ions. We believe that the reaction obeys the following equations:

$$V_2O_5+Y_2O_3 \rightarrow 2YVO_4 \quad (1)$$

$$Ce_2(CO_3)_3 \rightarrow Ce_2O_3 + 3CO_2 \uparrow \qquad (900\ ^\circ C) \qquad (2)$$

$$xCe_2O_3 + V_2O_5 + (1\text{-}x)Y_2O_3 \rightarrow 2Y_{1\text{-}x}Ce_xVO_4 \qquad (3)$$

The concentrations of Ce^{3+} ions in YVO_4 single crystal vary from x=0.005 to x=0.06. The process of crystal growth has been reported in our previous work [6].

The X-ray diffraction (XRD) was measured at room temperature and performed by a Rigaku D/max 2500v/PC diffractometer in the 2θ range from 10° to 90° in a step scan mode, with steps of 0.02°, using CuKα radiation of wavelength 0.154056 nm (40 Kw/200mA).

Fig. 1 Schematic diagram of the experiment equipment for crystal growth. The experiment equipment is composed of vacuum device (a rotary and a diffusion pump) and growth chamber.

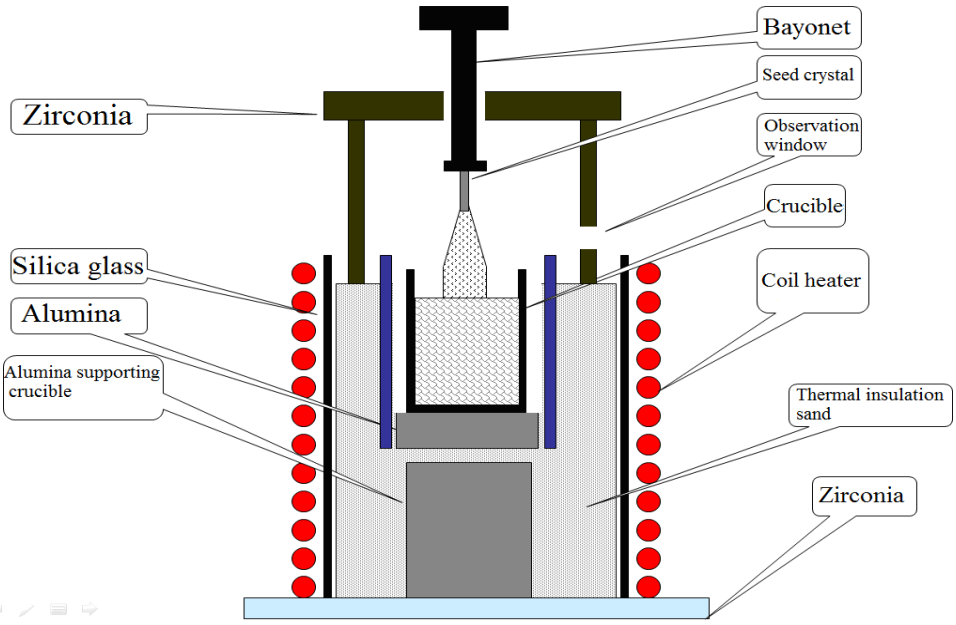

Fig. 2 Furnace designed for the crystal growth in the growth chamber.

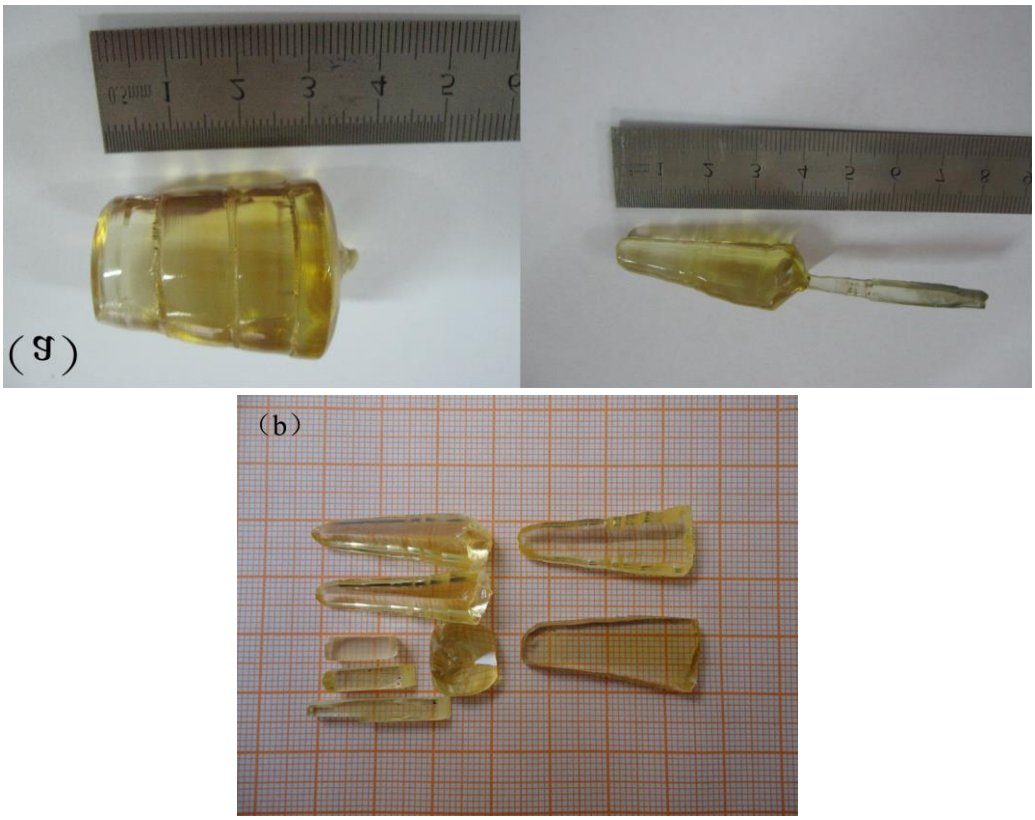

Fig. 3 Photographs of as-grown undoped YVO_4 single crystals (a) and cracks in the YVO_4 crystal (b). The cracks always occur parallel to the (100) and (010) planes.

Table 1 Characterization of the YVO4 single crystal.

Space group	D_{4h}^{19} - $I4_1$		
Crystal morphology	tetragonal		
Cell parameters	a=b= 7.12 Å, c= 6.29 Å		
Melting point	1825 ℃		
Density	4.22 g/cm		
Moh's hardness	~5		
Thermal expansion coefficient	a_a=4.43×10^{-6} /K	ac=11.37×10^{-6} /K	
Thermal conductivity	c-axis: 0.0523 W. cm/K	a-axis: 0.0510 W. cm/K	
Spectral transmission range	0.45~5 μm		
Sellmeier equation(λ: μm)	no^2 =3.77843+0.069736/(λ^2-0.04724)-0.0108133λ^2 ne^2 =4.55905+0.110534/(λ^2 -0.04813)-0.0122676λ^2		
Refractive index no	1.9929	1.9500	1.9447
Refractive index ne	2.22154	2.1554	2.1486
Birefringence(△n= n_e-n_o)	0.2225	0.2054	0.2039
Thermooptical coefficient	dn_a / dt=8.5×10^{-6} /K, dnc / dt=3.0×10^{-6} /K		

Fig. 3 (a) show the photographs of as-grown undoped YVO_4 single crystals grown by the Czochralski method in a medium frequency induction furnace, respectively. The YVO_4 single crystal is tetragonal with space phase of D_{4h}^{19} - $I4_1amd$ [4, 7]. The properties of YVO_4 single crystal are shown in Table 1. It can be found that the thermal conductivity of YVO_4 crystal is much smaller than the YAG crystal. In the process of crystal growth, the crystals sometimes cracks along the (100) and (010) planes. The high thermal stress is the main reason that causes the crystal to crack along the certain planes, which are seen as the cleavage planes. Fig. 3(b) shows the photographs of crystal cracking along the cleavage planes. The interplanar spacing for tetragonal crystal can be calculated as following formula:

$$\frac{1}{d_{hkl}} = \sqrt{\frac{h^2 + k^2}{a^2} + \frac{l^2}{c^2}} \tag{4}$$

Where a, b, c and β are lattice parameters. h, k and l are Miller indices. d_{hkl} is the interplanar spacing. According to the equation (4), the interplanar spacing values for the main planes are presented in table 2.

Table 2 Values of the interplanar spacings (d_{hkl}) for the main planes.

(hkl)	(100)	(010)	(001)	(111)	(011)	(110)	(021)	(-111)	(130)	(041)
dhkl/nm	0.7119	0.7119	0.6290	0.3930	0.4714	0.5034	0.3098	0.3930	0.2251	0.1713

As seen from table 2, the interplanar spacings for the (100) and (010) planes are larger than that of other planes. The larger interplanar spacing means that the inter-atomic bonding forces perpendicular to the (010) plane or (100) plane are much weaker. The major factor of crystal cracking is the high thermal stress. However, the temperature gradient, growth rate and cooling rate have strong effects on the thermal stress [8]. In order to obtain the high-quality YVO_4 crystal, choosing the appropriate temperature gradient, growth rate and cooling rate plays a very important role in the crystal growth. Fig. 2 shows

2.1 Effect of the temperature gradient on crystal cracking

The axial temperature gradient in the furnace is the driving force of the crystal growth, while the large temperature gradient usually results in the thermal stress and relative deformation in crystal, which lead to the crystal cracking. Brice pointed out that the allowable maximum axial temperature gradient of no cracking crystal ($G_{\max}$) is approximate to the following formula [9]:

$$G_{\max} = \frac{2\varepsilon_b}{\alpha R^{3/2}} \left(\frac{2}{h}\right)^{1/2} \tag{5}$$

Where ε_b is the fracture strain of the crystal (the allowable maximum stress must be smaller than ε_b), α is the thermal expansion coefficient, h is the heat exchange coefficient, R is the radius of the crystal.

It is obvious that the allowable maximum axial temperature gradient is directly proportional to $\frac{1}{R^{3/2}}$ and ε_b. In order to ensure the allowable maximum stress is smaller than ε_b, the axial temperature gradient needs to be reduced as the crystal radius increases. Because the temperature gradient is the driving force of crystallization, the much smaller temperature gradient is not better. According to the actual experiment, when the radius of the crystal is 5 mm, the optimum axial temperature gradient is 7 °C/mm. In addition to the axial temperature gradient, the radial temperature gradient also exists in the furnace. To restrain some unexpected spontaneous nucleation actions as a result of the large temperature difference at the solid-liquid interface, the much smaller radial temperature gradient is better. That can keep the warmth of crystal and prevent the crystal from cracking.

2.2 Effect of growth rate on crystal cracking

The boundary condition at the solid-liquid interface for heat transport is given by the interfacial heat balance equation [10]:

$$\rho_s \omega_{s,i} Hf = K_{s,i} G_{s,i} - K_{l,i} G_{l,i} \tag{6}$$

Where s, l and i mean solid, liquid and solid-liquid interface, respectively. G is the temperature gradient, K is the thermal conductivity of crystal, L is the latent heat of cryallization, ρ_s is the density of crystal, $\omega_{s,i}$ is solid concentration, H is the fusion enthalpy, f is the growth rate.

In Eq. (6), the growth rate is determined by the axial temperature gradient. During the crystal growth, solid layer thickness increases with time. In order to promote the crystal growth rate (f), the temperature gradient in crystals ($G_{s,i}$) must be raised or the much smaller temperature gradient in melt ($G_{l,i}$) can be applied to growing the crystal. However, the greater temperature gradient ($G_{s,i}$) leads to the higher thermal stress. Taking into account the effect of thermal stress on the crystal cracking, the allowable maximum thermal stress $\delta_{\max}$ is given by the following equation:

$$\delta_{\max} = \frac{1}{4}\alpha R(hR)^{1/2}\left(1-\frac{1}{2}hR\right)^{-1} G_{s,i} \tag{7}$$

In Eq. (7), α is the thermal expansion coefficient, h is the heat exchange coefficient, R is the radius of the crystal.

As seen from Eqs. (6) and (7), the maximum thermal stress ($\delta_{\max}$) is proportional to the growth rate (f). The slow growth rate can contribute to obtaining the high-quality crystal. This point is very important for the doped crystal. When the dopants enter into YVO_4 crystal and occupy the certain lattice sites, it causes the lattice distortion. The higher Ce^{3+} ions are doped in the crystal, the more severe lattice distortion is. The crystal with severe lattice distortions usually can not endure the high internal stress and result in cracking. Based on the experimental equipment and experience, the growth rate 1.5-2.0 mm/h is applied to the growth of the crystals. Meanwhile, the crystal rotation speed is about 20-25 r/min.

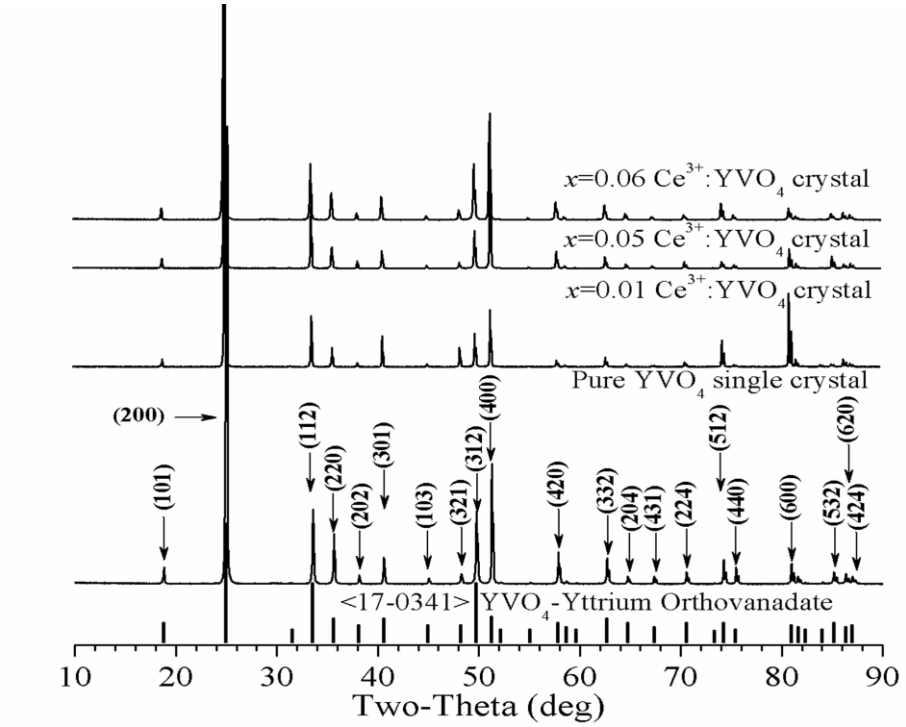

Fig. 4. XRD patterns of the pure YVO_4 and Ce^{3+}-doped YVO_4 crystals.

2.3 Effect of cooling rate on crystal cracking

Cooling stage is the final stage of the crystal growth. If the cooling rate is too fast, the relative deformations will occur in the crystal. The relative deformations produce the high thermal stress leading to the crystal cracking. The largest cooling rate can be defined as following formula:

$$\left(\frac{dT}{dt}\right)_{\max} = \frac{4\sqrt{2}}{\alpha R^2} K\varepsilon_b \tag{8}$$

Where α is the thermal expansion coefficient, K is the thermal diffusion coefficient, R is the radius of the crystal. The allowable maximum cooling rate is inversely proportional to the thermal expansion coefficient (α). The YVO_4 and Ce^{3+}-doped YVO_4 single crystals require slow cooling rate to recover its shape steadily. In order to reduce the cooling rate, the final cooling rate is less than 15 K/h and the whole period of crystal growth is about 36 hours.

Fig. 4 shows the XRD patterns of the pure YVO_4 and Ce^{3+}-doped YVO_4 crystals. The strong XRD peaks are collected in a wide angle range and some evident peaks are assigned. The diffraction peaks and relative intensity agree well with the standard data of YVO_4 (JCPDS card No. 72-0341), which indicates that the obtained phase is YVO_4 without any parasitic phase, such as the Y_2O_3 or V_2O_5 phases. The Ce^{3+} ions enter into the YVO_4 crystal and occupy the Y^{3+} lattice sites. The ionic radii of Ce^{3+} and Y^{3+} ions are 0.102 nm and 0.1015 nm [11-13], respectively. It is obvious that the radius of Ce^{3+} ions is very similar to that of the Y^{3+} ions so that the lattice distortion caused by Ce^{3+} ions is very small, which contributes to the crystal growth.

3. Conclusion

In summary, the high-quality YVO_4 and Ce^{3+}-doped YVO_4 single crystals were grown by the Czochralski method. Based on the theoretical analysis, experimental equipment and experience, high thermal stress is the major fact of crystal cracking along the cleavage planes. The stress is determined by the gradient temperature, growth rate and cooling rate. The optimal growth parameters have been obtained as follows: the axial gradient temperature is 7 K/mm, the growth rate is 1.5-2.0 mm/h, the crystal rotation speed is about 20-25 r/min, the final cooling rate is less than 15 K/h.The whole period of crystal growth is about 36 hours. Finally, the X-ray diffraction (XRD) patterns indicated that the obtained phase was YVO_4 without any parasitic phase.

Acknowledgements

We thank Wenrun Li, Liangang Li and Zhouli Wu at Tianjin University for providing the help.

References

[1] E.B. Roch, J. Phys. Chem. 20, 345 (1933).
[2] J.J. Rubin, L.G. Van Uitert, J. Appl. Phys, 37,2920 (1996).
[3] R.A. Fields, M. Birnbaum, C.L. Fincher, Appl. Phys. Lett. 51, 1885 (1987).
[4] H.H. Yu, H.J. Zhang, J.Y. Wang, Acta Physica Polonica A, 124 (2013).
[5] B.Q. Hu, Y.Z. Zhang, X. Wu, X.L. Chen, Journal of Crystal Growth, 226, (2001) 511-516.
[6] Y.F. Wang, S. Wang, Z.L. Wu, W.R. Li, Y.F. Ruan, J. Alloys Comp. 551 (2013) 262.
[7] H.R. Xia, X.L. Meng, M. Guo, L. Zhu, H.J. Zhang, J. Y. Wang, J. Appl. Phys. 88, 5134 (2000).
[8] G.Y. Zhang, T.C. Chong, X.W. Xu, H. Kumagai, Journal of Crystal Growth 225 (2001) 495.
[9] J.C. Brice, Journal of Crystal Growth 42 (1977) 427.
[10] K. Fukui, K. Maeda, Chemical Engineering Science 57 (2001) 3133.
[11] S. Wang, Y.F. Ruan, T.J. Tsuboi, H.S. Tong, Y.F. Wang, S.C. Zhang, Physica B 431 (2013) 37.
[12] R.D. Shannon, Acta Crystallogr. A 32 (1976) 751.

[13] S.C. Zhang, Y.F. Ruan, G.Z. Jia, Z.H. Feng, Z.P. Liu, L.B. Pei, Journal of Inorganic Materials 29 (2014) 1067.